Macromolecular Rapid Communications
www.mrc-journal.de

Polyether-Based Diblock Terpolymer Micelles with Pendant Anthracene Units—Light-Induced Crosslinking and Limitations Regarding Reversibility

*Johanna K. Elter, Jonas Eichhorn, and Felix H. Schacher**

The synthesis of 9-methylanthracenyl glycidyl ether (AnthGE) as a crosslinkable monomer that can be applied in anionic ring opening polymerization is reported. Diblock terpolymers of the composition methoxy-poly(ethylene oxide)-*block*-poly(2-ethylhexyl glycidyl ether-*co*-9-methylanthracenyl glycidyl ether) (mPEO-*b*-P(EHGE-*co*-AnthGE) with 10 to 24 wt% of AnthGE are synthesized and characterized. Their micellization behavior, as well as their light-induced core-crosslinking via irradiation with UV light ($\lambda = 365$ nm) is studied. The results are compared with studies on the dimerization, and the dimer cleavage via irradiation with UV–C light ($\lambda = 254$ nm), of the same diblock terpolymer in organic solution, and the small-molecule model compound 9-methoxymethylanthracene. Differences in ^{1}H NMR spectra of the crosslinked or dimerized compounds and reaction kinetics of the dimerization reactions under different conditions suggest possible side reactions for the case of the core-crosslinking of micelles in aqueous solution. These side reactions limit the reversibility of the anthracene dimerization reaction in aqueous solutions, even if the anthracene molecule is encapsulated within the hydrophobic core of a polymeric micelle.

1. Introduction

In recent years, micellar systems generated from block copolymers gained increasing attention as they can be applied for a variety of purposes, including drug delivery,[1,2] waste water treatment via encapsulation of metal ions,[3,4] or nanocontainers for catalysis under confinement.[5,6] Especially micelles formed from amphiphilic block copolymers in aqueous solutions are of interest, as water solubility is required for biological applications and can also be desired in catalysis to reduce the application of potentially toxic organic solvents.[7] As block copolymers are versatile structures, micelles can be tailor-made to suit the specific purpose of their application. By choosing suitable monomer combinations and architectures[8] and controlling molecular weight (M_n) and dispersity ($Đ$),[9,10] the self-assembly of polymeric materials can be controlled and additional functionalities can be introduced into the micelle.[11,12]

Nevertheless, for many applications, micelles have to exhibit a certain degree of stability to prevent disassembly of the structures at an undesired time point.[13] Disassembly could happen due to dilution below the critical micellization concentration,[14] changes in pH value of the surrounding solvent[15] or small molecules present in the micellar environment.[16] Further, disassembly during purification or recirculation processes is possible. To avoid these problems, core or shell crosslinking is a suitable approach to stabilize micellar systems. Up to date, a large amount of different crosslinking strategies is described in literature.[13,17,18] One of the simplest approaches probably is the photopolymerization of alkene units present in the polymer side chain, yet this method has several drawbacks: The degree of crosslinking is not easily trackable, and the crosslinking reaction is not reversible.[19,20] Reversibility and adjustability can be achieved by, for example, using furan units as crosslinkable moieties and encapsulating a bismaleimide crosslinker beforehand.[21,22] Furan and maleimide units undergo Diels–Alder reactions at low to moderate temperatures which are thermally reversible.[23] In other systems, the formation of imines from amines and aldehydes[24] or hydrazones from hydrazines and aldehydes[25] present two types of linkages which can be created and cleaved upon changes in pH. However, small molecule crosslinkers may suffer from inefficient encapsulation and unreacted crosslinker molecules may be a problem in some applications. Therefore, a combination of the advantages of both methods is desirable.

The incorporation of light-responsive units into block copolymer micelles was first reported by Wang et al. in 2004. In that case, azobenzene units were incorporated into the core-forming block to change its hydrophilicity via light-induced

J. K. Elter, J. Eichhorn, F. H. Schacher
Institute of Organic Chemistry and Macromolecular Chemistry
Friedrich Schiller University Jena
Humboldtstraße 10, Jena D-07743, Germany
E-mail: felix.schacher@uni-jena.de
J. K. Elter, J. Eichhorn, F. H. Schacher
Jena Center for Soft Matter (JCSM)
Friedrich Schiller University Jena
Philosophenweg 7, Jena D-07743, Germany

DOI: 10.1002/marc.202100485

E/Z-isomerization.[26] Similar effects can be achieved via the incorporation of spiropyranes.[27,28] This concept of reversibly tuning micellar properties via irradiation with light can further be applied to covalent crosslinking, for example by incorporation of coumarin side groups into the core or the shell of a polymeric micelle.[29] UV-irradiation at $\lambda > 310$ nm allows for the dimerization ([2+2]-cycloaddition) of two coumarin units, while irradiation at $\lambda < 260$ nm reverses this process.[30] Cinnamate and its derivatives can be applied in a similar way.[31] Further, stilbene moieties can be dimerized via irradiation with UV-light, for example for the generation of polymeric nanowires.[32,33] Another well-investigated reaction is the UV-induced dimerization ([4+4]-cycloaddition) of anthracene at $\lambda > 350$ nm, and the subsequent dimer cleavage at $\lambda < 250$ nm.[34–36] This reaction was already applied for crosslinking or self-healing of polymer films,[37,38] the connection of two homopolymers for block copolymer formation,[39] or the generation of crosslinked particles in organic solution.[40] Depending on the system and the light source used for irradiation, this dimerization is reversible.[40,41] Another benefit of using this reaction for polymer crosslinking is the possibility to determine the degree of crosslinking easily via UV–vis spectroscopy. Nevertheless, complete dimer cleavage is not possible in many cases, a fact that can be attributed to several side reactions, depending on the chemical environment,[42,43] as well as to an overlap of wavelengths that can cause dimerization, or dimer cleavage. While this does not hamper possible applications such as the generation of shape-memory polymers,[38,44] it can be problematic for polymeric micelles that should be crosslinked, and afterwards de-crosslinked completely to trigger disassembly—most studies focusing on micelles in aqueous systems that can be crosslinked via anthracene dimerization do not focus on the reversibility of this reaction.[45] An alternative to the dimer cleavage via UV–C light is the thermal cleavage of the anthracene dimer, which was reported for several small-molecule compounds as well as for anthracene moieties incorporated into polymers.[46,47] Yet, also the thermal cleavage reaction suffers from limitations, as the required temperatures depend on the substituents and the stereochemistry of the cycloadduct, but are often rather high (>130 °C).[36,46,48] Therefore, thermally labile or reactive groups must not be present in the polymer. Further, the application of water as a solvent, for example for crosslinked micellar systems, is in such cases only possible if the reaction is carried out under pressure.

In this study, we present the synthesis of 9-methylanthracenyl glycidyl ether as a novel monomer suitable for anionic ring opening polymerization (AROP), which can be incorporated into polyether-based amphiphilic diblock terpolymers. These diblock terpolymers can be purified easily via dialysis, resulting in final products of the structure methyl-poly(ethylene oxide)-*block*-poly(2-ethylhexyl glycidyl ether-*co*-9-methyl-anthracenyl glycidyl ether) (mPEO-*b*-P(EHGE-*co*-AnthGE)) that contain up to 24 wt% of AnthGE. Polyether-based block copolymers are versatile structures that open up the possibility to incorporate a variety of side groups and functionalities into a flexible polymer chain. We aim to introduce anthracene as light-responsive side group for this class of polymers and evaluate the scope as well as the limitations of the UV-induced [4+4]-cycloaddition of two anthracene units at $\lambda = 365$ nm for crosslinking before and after self-assembly in aqueous solution. While this crosslinking process is shown to be partially reversible upon irradiation with UV–C light ($\lambda = 254$ nm) for the unimolecularly dissolved diblock terpolymer in degassed, water-free environment (dichloromethane, DCM), crosslinking of the polymeric micelles is permanent to a large extent. Thermal cleavage of the anthracene dimer was not investigated, as the PEO-stabilized micelles precipitate from aqueous solutions at temperatures >120 °C due to the LCST behavior of PEO and PEO-based polymers.[49] Analysis of the crosslinking reaction via UV–vis and ^{1}H NMR spectroscopy suggests that side reactions cannot be excluded even in degassed aqueous environments. As one example, the formation of anthraquinone as a side product of the crosslinking reaction can be observed. Further, irreversible core-crosslinking of the micelles may be attributed to photo-oxidation of the anthracene units, which allows for the dimerization of two anthracene molecules upon addition of water.[42]

2. Results and Discussion

2.1. Diblock Terpolymer Synthesis

The synthesis of the diblock terpolymers was carried out using commercially available poly(ethylene oxide) monomethyl ether (mPEO) as macroinitiator for AROP. To attach the second, hydrophobic block, mPEO was dissolved in dry benzene, the free hydroxyl group was deprotonated using NaH for 2 h at 110 °C, and the glycidyl ether monomers were added subsequently. We used a mixture of the commercially available 2-ethyl hexyl glycidyl ether (EHGE) and 9-methylanthracenyl glycidyl ether (AnthGE), which was synthesized from 9-anthracenecarboxylic acid as described in the Experimental Section. The polymerizations were allowed to proceed for 48 h at 110 °C before they were quenched by addition of ethanol (EtOH, **Scheme 1**). Polymerization using potassium as a counter ion, which would allow for lowering the reaction temperature, was not possible, presumably due to unfavorable interactions between the metal cation and the anthracene moieties.[50] The latter interactions as well as a low reactivity of AnthGE may also be a reason for incomplete monomer conversion. As precipitation of the diblock terpolymer was not suitable as purification procedure, residual monomer and low molecular weight side products[51] were removed via dialysis against tetrahydrofuran (THF) using regenerated cellulose (RC) dialysis tubes (molecular weight cut-off (MWCO) = 6000–8000 kDa) after polymerization. The molar masses, dispersities, and compositions of the diblock terpolymers are given in **Table 1**. Size exclusion chromatography (SEC) traces and ^{1}H NMR spectra are shown in **Figure 1**. The assignment of the ^{1}H NMR signals can be found in Figure S1, Supporting Information.

2.2. Dimerization of the Anthracene Side Group

Despite the fact that the light-induced [4+4]-cycloaddition of two anthracene units as well as the cleavage of the resulting anthracene dimer (**Scheme 2**) is well-studied, numerous variables can influence the dimerization reaction. The chosen light source and irradiation wavelength, the concentration of anthracene units and the chemical environment (substituents as well as solvents or matrix) are important parameters. While substituents attached to the anthracene rings can influence their reactivity, small

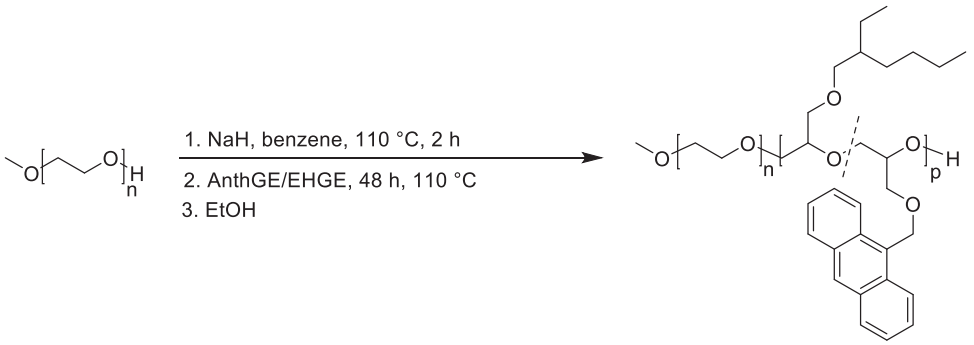

Scheme 1. Synthesis of the diblock terpolymers via re-initiation of a PEO macroinitiator and subsequent AROP of glycidyl ethers from the latter.

Table 1. Molar mass (M_n), dispersity ($Đ$), and composition (degree of polymerization, *DP*, and weight fraction, wt%) of the macroinitiator mPEO-OH and the three different diblock terpolymers. The *DP* is highlighted in red in the table presenting the diblock terpolymer compositions.

Polymer	M_n (^{1}H NMR) [g mol^{-1}]	M_n (SEC[a)]) [g mol^{-1}]	$Đ$ [SEC[a)]]	Composition (*DP*) / [wt%]					
				EO		EHGE		AnthGE	
mPEO-OH	n.d.	5000	1.08	114	100	0	0	0	0
mPEO-*b*-P(EHGE-*co*-AnthGE)	13 300	7200	1.17	114	38	27	38	12	24
	11 800	6800	1.19	114	43	23	36	9	21
	8100	6100	1.17	114	64	11	26	3	10

[a)] $CHCl_3$/NEt_3/iPrOH 94:4:2, PEO-Calibration

molecules like oxygen or water in the reaction mixture can cause side reactions that are competing with the dimerization reaction. Therefore, it is recommendable to investigate the reactivity of the investigated system instead of exclusively relying on existing kinetic studies of similar systems. We investigated the dimerization and cleavage of the anthracene units present in our diblock terpolymers in solution via UV–vis and ^{1}H NMR spectroscopy. To generate a better understanding for the influence of the polymeric backbone on the dimerization process, we compared the data with results obtained for the anthracene-containing glycidyl ether monomer as well as for 9-methoxymethylanthracene. The latter was chosen as a model substance for irradiation experiments due to the limited stability of the epoxide group during irradiation experiments with UV–C light (λ = 254 nm).

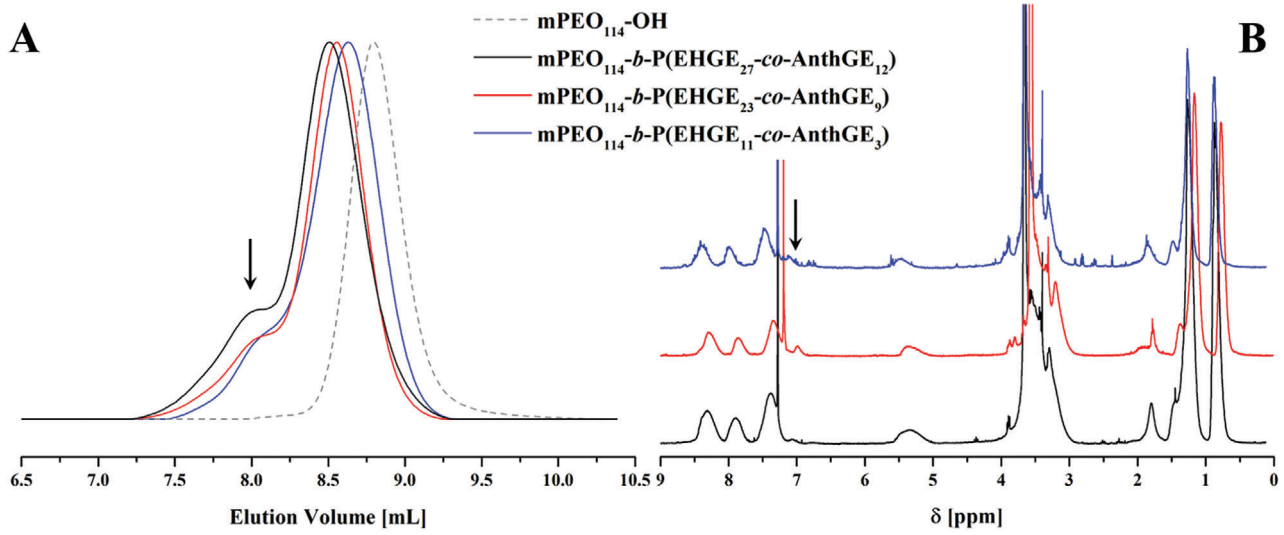

Figure 1. A) SEC traces and B) ^{1}H NMR spectra of the diblock terpolymers presented in Table 1. The shoulder that is visible in the SEC traces (black arrow) corresponds to species with twice the molar mass of the product and presumably originated from intermolecular anthracene dimerization during polymerization, as visible also in ^{1}H NMR spectra, as well as from PEO species containing two hydroxyl groups that are present in the PEO macroinitiator that are able to initiate block extension on both chain ends.

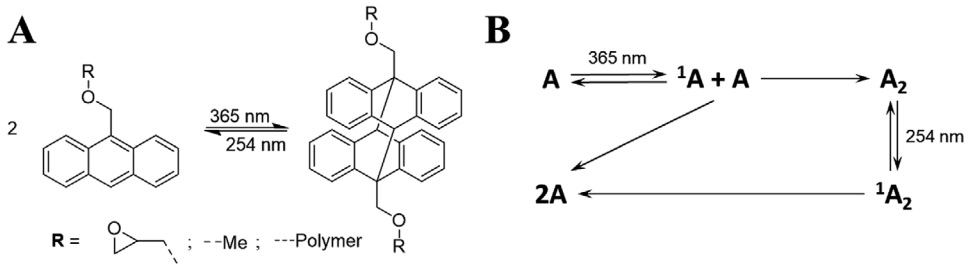

Scheme 2. A) UV-induced dimerization, or [4+4]-cycloaddition, of two anthracene units with different substituents at $\lambda = 365$ nm, and subsequent dimer cleavage at $\lambda = 254$ nm. B) Kinetic description of the reaction under the assumption that no side reactions are taking place.[52] A = anthracene unit, A_2 = anthracene dimer, $^1A/^1A_2$ = excited (singlet state) anthracene unit or anthracene dimer.

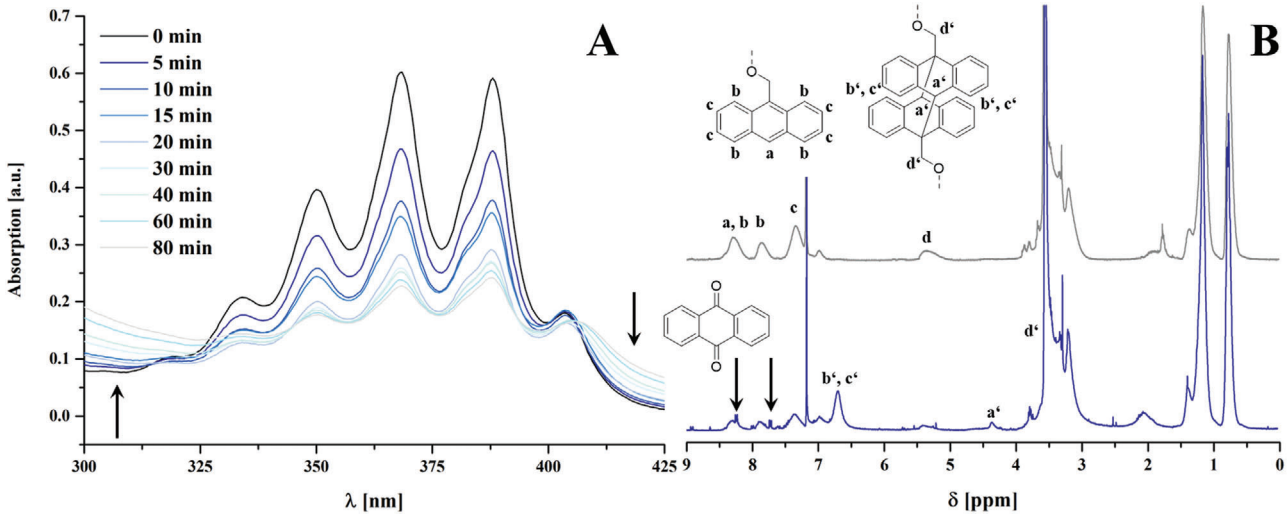

Figure 2. A) Time-dependent UV–vis spectra of $mPEO_{114}$-*b*-P($EHGE_{23}$-*co*-$AnthGE_9$) during the irradiation at $\lambda = 365$ nm, and B) ^{1}H NMR spectra before (grey) and after (blue) irradiation. The increase of the absorption marked with the black arrows in picture (A), as well as the ^{1}H NMR signals at 8.34 and 7.83 ppm, indicate the formation of anthraquinone as a side product of the reaction. *C* (reaction solution, DCM) = 3 mg mL^{-1}; *c* (UV–vis, DCM) = 0.25 mg mL^{-1}.

Cycloaddition reactions of the monomer and the model compound were carried out in DCM solution at a concentration of 3 mg mL^{-1}. All solutions were degassed with argon for 10 min prior to irradiation at $\lambda = 365$ nm, as the presence of oxygen led to 9,10-addition of the latter (Figure S2, Supporting Information). The reactions were monitored via UV–vis spectroscopy and followed a first order rate law, as shown in Figure S3, Supporting Information, for 9-methoxymethylanthracene. After 180 min, the absorption at 365 nm decreased to ≈20% of the starting value (80% conversion) for both 9-methoxymethylanthracene and AnthGE, while ^{1}H NMR spectra suggested a lower conversion of 65% for 9-methoxymethylanthracene, and 71% for AnthGE (Figure S4, Supporting Information).

As the reversibility of the dimerization was of special interest for the later formation of reversibly crosslinkable block copolymers and block copolymer micelles, the cleavage of the dimer, which is reported to occur under irradiation at 254 nm, was investigated. UV–vis studies as well as ^{1}H NMR experiments showed that roughly 60% of 9-methoxymethylanthracene was recovered, while the other 40% were still present in the solution as dimers (Figure S5, Supporting Information). Longer reaction times did not lead to increased dimer cleavage, but to decomposition reactions. As long as dimer cleavage was observed as the dominant process, the reaction followed a first order rate law. Further, it has to be mentioned that dimerization at 254 nm cannot be excluded completely, as 9-methoxymethylanthracene also shows UV–vis absorption in this region.[53] The investigation of the cleavage of AnthGE dimers was not possible due to side reactions of the epoxide group upon irradiation at $\lambda = 254$ nm.

Even if the light response of anthracene units, and therefore also of anthracene-containing polymers, may be limited under the given conditions, literature suggests that it is not compulsory to achieve full conversion in crosslinking and decrosslinking reactions for every possible application of a crosslinked material.[44] Therefore, investigation of the cycloaddition reaction and dimer cleavage of anthracene units incorporated in a diblock copolymer may still yield interesting results.

To investigate dimerization of the diblock terpolymers, $mPEO_{114}$-*b*-P($EHGE_{23}$-*co*-$AnthGE_9$) was used as model compound. The diblock terpolymer was dissolved in DCM at a concentration of 3 mg mL^{-1} and the solution was degassed before irradiation was started. Within 80 min, 65% of the anthracene units were consumed according to UV–vis spectroscopy (**Figure 2**A). ^{1}H NMR spectroscopy suggested a higher value

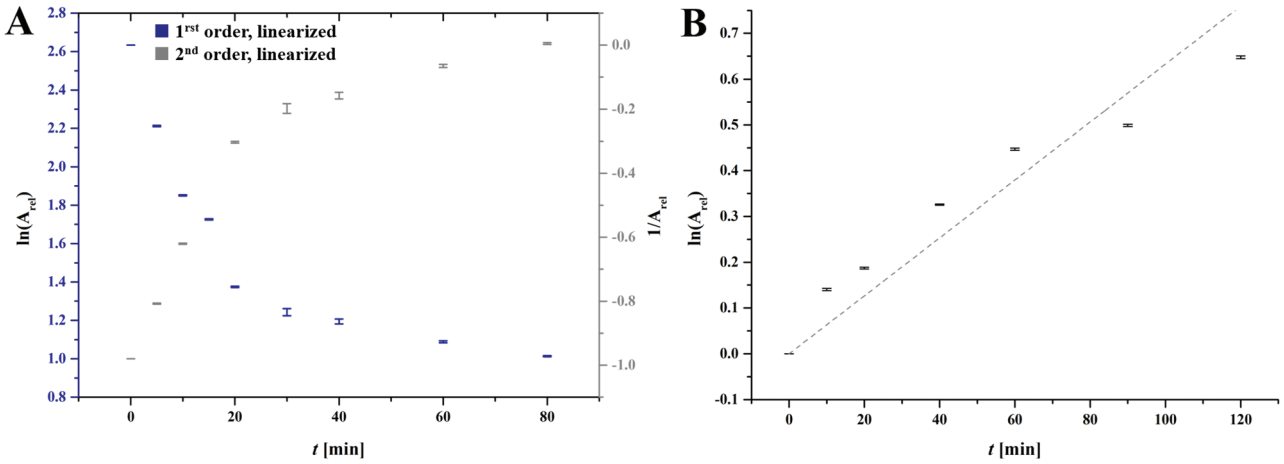

Figure 3. A) Plots of $\ln(A_{rel})$ and $1/A_{rel}$ versus time for the dimerization of anthracene units incorporated into $mPEO_{114}$-*b*-P($EHGE_{23}$-*co*-$AnthGE_9$) via irradiation at $\lambda = 365$ nm in DCM solution. In both cases, no linear fit describing a rate law of either first order ($\ln(A_{rel})$) or second order ($1/A_{rel}$) is possible. B) In contrast, the dimer cleavage can be described with a first order reaction law for this case. $A_{rel} = A/A_0$, $\lambda = 367$ nm.

of ≈75% (Figure 2B). Nevertheless, it has to be mentioned that this was not completely due to dimerization. Despite the fact that dry solvents were used, and the solution was degassed prior to irradiation, the formation of anthraquinone as a side product was detectable (Figure 2, black arrows). This may also cause the discrepancy between the detected consumption of anthracene units in UV–vis and ^{1}H NMR, as anthraquinone shows absorption in a similar region as anthracene.[54] It is possible that traces of water, which were not possible to remove from the diblock terpolymer while drying under high vacuum, caused the side reaction. In non-dried, protic solvents, for example methanol (MeOH), anthraquinone formation becomes prominent compared to the anthracene dimerization reaction (Figure S6, Supporting Information).

Surprisingly, no changes were detected in SEC traces after the dimerization process (Figure S7, Supporting Information). A possible explanation for this is that only intramolecular dimerization took place, as anthracene units connected to the same polymer chain are already in close proximity to each other, which is required for the cyclization reaction. A strong broadening of the fluorescence spectrum compared to the small-molecule anthracene derivatives supports this finding (Figure S8, Supporting Information).[55] At this point it should be mentioned that dimerization and dimer cleavage reactions can also be followed via fluorescence spectroscopy; the results were in agreement with the results obtained via UV–vis and ^{1}H NMR spectroscopy. Exemplary fluorescence spectra obtained during irradiation experiments are presented in Figure S9, Supporting Information. Concentration-time-profiles further show that in contrast to the cyclization of small-molecule anthracene compounds, no first order rate law can be applied. A possible reason for this is that only anthracene units that are already pre-ordered within one polymer chain can react freely. For other anthracene units, the rate determining factor may be diffusion and arrangement, as perfect mixing of the anthracene units cannot be assumed when they are connected to a polymeric backbone (**Figure 3**A).[56]

In contrast, the dimer cleavage should not directly be hampered by attachment of the anthracene units to a polymer backbone. Here, UV–vis spectra suggest the recovery of 70% of the anthracene units (**Figure 4**A). The reaction follows a first order rate law, equally to the behavior found for small molecule anthracene dimers (Figure 3B). In contrast, ^{1}H NMR investigations do not only show the decrease of the intensity of the proton signals corresponding to the anthracene dimers, but also the appearance of a shoulder in the range between 7.4 and 7.0 ppm, which hampers exact detection of the amount of recovered anthracene units (Figure 4B).

Hence, it has to be assumed that side reactions occurred. Irradiation times longer than 120 min led to the decrease of the anthracene peaks in UV–vis spectra, again suggesting that side and decomposition reactions become more prominent.

2.3. Application of Anthracene Dimerization for Micellar Crosslinking

In the next step, we investigated whether the light-induced dimerization of anthracene and the dimer cleavage are suitable to generate reversibly core-crosslinked micelles from the presented diblock terpolymers. All diblock terpolymers listed in Table 1 formed micelles via self-assembly in aqueous solution. The micelles were prepared via generation of a thin polymer film by drying a solution of the respective diblock terpolymer in THF, and subsequent rehydration of the latter. The final concentration of the diblock terpolymers in water was 1 mg mL^{-1}. As dynamic light scattering (DLS) investigations indicated the formation of non-spherical aggregates from $mPEO_{114}$-*b*-P($EHGE_{23}$-*co*-$AnthGE_9$) and $mPEO_{114}$-b-P($EHGE_{27}$-*co*-$AnthGE_{12}$), additional cryogenic transmission electron microscopy (cryo-TEM) measurements were performed to determine morphology and size of the solution structures (**Figure 5** and **Table 2**).

For $mPEO_{114}$-*b*-P($EHGE_{23}$-*co*-$AnthGE_9$) and $mPEO_{114}$-*b*-P($EHGE_{27}$-*co*-$AnthGE_{12}$), mixed phases of spherical micelles and vesicles were found. For $mPEO_{114}$-*b*-P($EHGE_{27}$-*co*-$AnthGE_{12}$), also worm-like micelles were detected. Besides the fact that traces of polymeric dimer are present during self-assembly, as

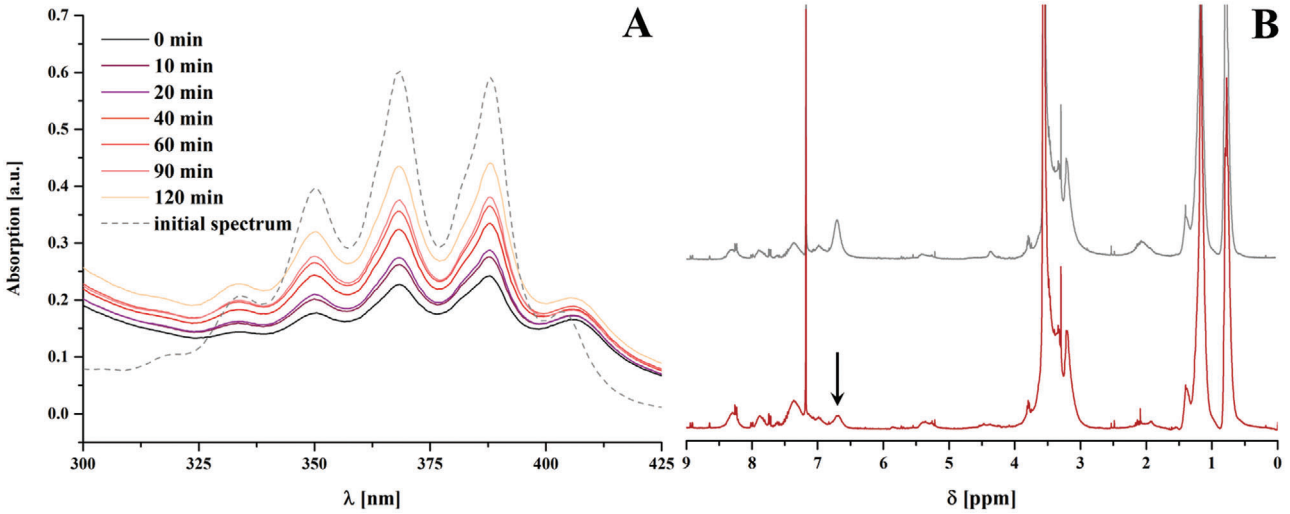

Figure 4. A) Time-dependent UV–vis spectra of $mPEO_{114}$-*b*-P($EHGE_{23}$-*co*-$AnthGE_9$) during the irradiation at $\lambda = 254$ nm and B) ^{1}H NMR spectra before (grey) and after (red) irradiation at that wavelength. UV–vis spectra indicate the incomplete cleavage of the anthracene cycloadducts. In ^{1}H NMR spectra, the signal at 6.8 ppm corresponding to the aromatic ring protons of the dimer decreased (black arrow).

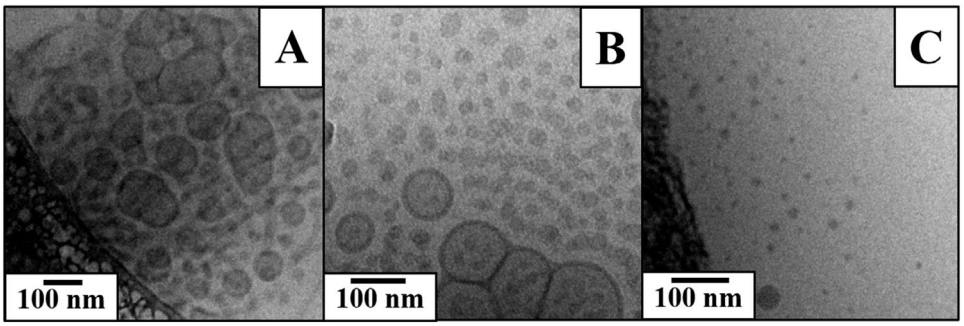

Figure 5. Cryo-TEM micrographs of A) $mPEO_{114}$-*b*-P($EHGE_{27}$-*co*-$AnthGE_{12}$), B) $mPEO_{114}$-*b*-P($EHGE_{23}$-*co*-$AnthGE_9$), and C) $mPEO_{114}$-*b*-P($EHGE_{11}$-*co*-$AnthGE_3$), $c = 1$ mg mL^{-1}.

it can be seen in SEC traces in Figure 1, the chosen preparation technique may also influence the obtained morphologies, as the film rehydration technique can favor the formation of vesicles. Further, the ability of anthracene to form π–π-stacks may influence the arrangement of polymer chains in the film as well as their behavior during micelle formation. For low AnthGE contents, these effects were less prominent. Due to that, and due to the overall lower *DP* of the hydrophobic block, $mPEO_{114}$-*b*-P($EHGE_{11}$-*co*-$AnthGE_3$) formed exclusively spherical micelles, as suggested by DLS measurements resulting in a hydrodynamic radius of 15 nm as the main population (Table 2 and Figure S10, Supporting Information).

For micellar crosslinking, the solutions were degassed with argon and subsequently irradiated at $\lambda = 365$ nm. Despite the lower overall concentration of anthracene units, the decrease of the respective peaks in the UV–vis spectrum of the micelles occurred faster, which was attributed to the fact that the anthracene units are already pre-arranged within the collapsed, hydrophobic core of the micelles (**Figure 6**A,B). DLS and cryo-TEM investigations showed no significant changes in the

Table 2. Hydrodynamic radii, core radii, and morphologies of the aggregates formed from the anthracene-containing diblock terpolymers.

Polymer	$<R_H>_{z,app}$ [a)] [nm]	r_{core} [b)] [nm]	Morphology [b)]
$mPEO_{114}$-*b*-P($EHGE_{27}$-*co*-$AnthGE_{12}$)	51	n.d.	Filomicelles, vesicles
$mPEO_{114}$-*b*-P($EHGE_{23}$-*co*-$AnthGE_9$)	14	31 ± 7	Spheres, vesicles
$mPEO_{114}$-*b*-P($EHGE_{11}$-*co*-$AnthGE_3$)	15	13 ± 3/63 ± 14	Spheres

[a)] determined via intensity-weighted DLS CONTIN plots; [b)] determined for the partition of spherical micelles via cryo-TEM by measuring at least 40 individual aggregates.

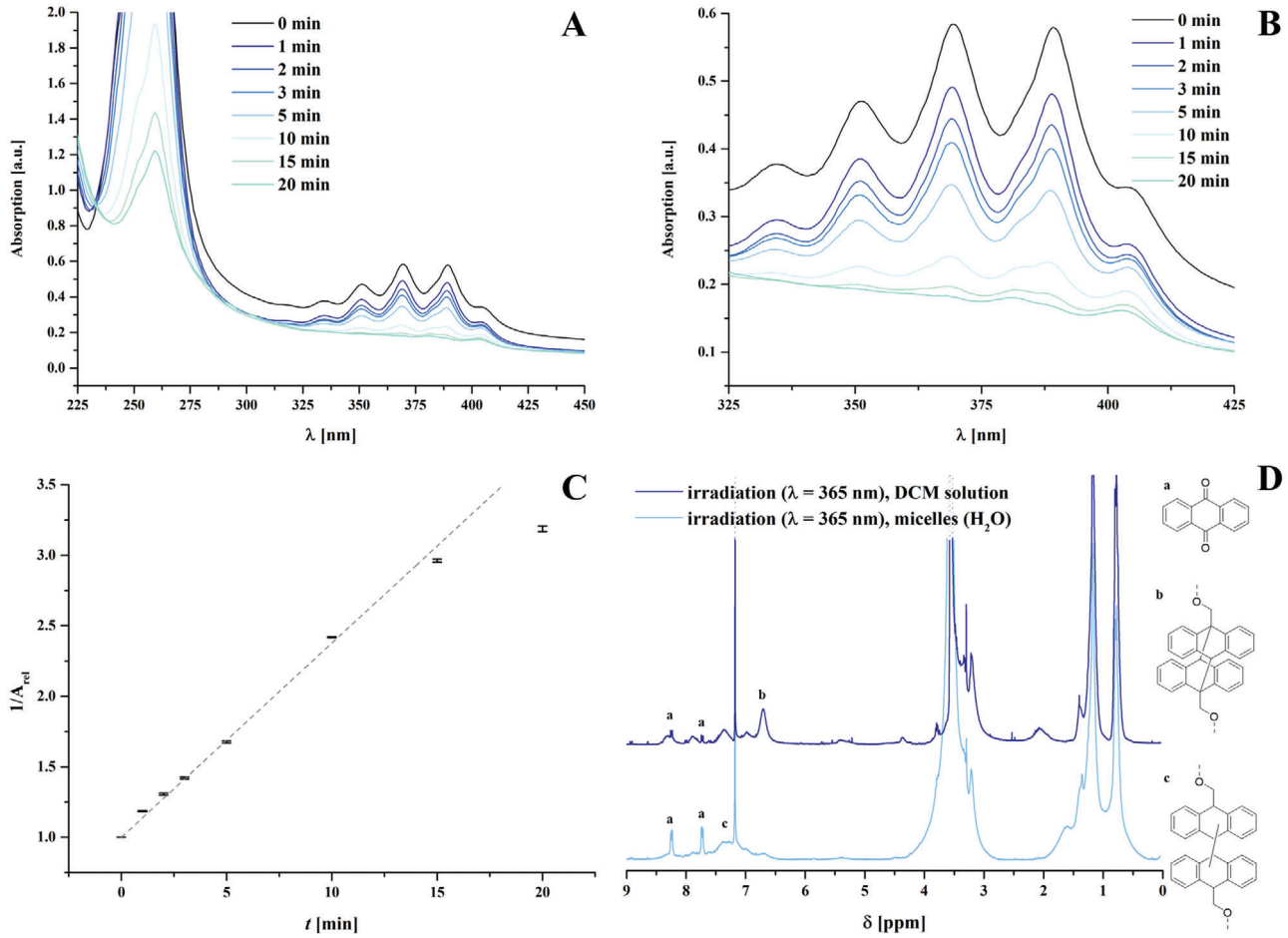

Figure 6. A,B) Time-dependent UV–vis spectra of micelles formed from $mPEO_{114}$-*b*-P($EHGE_{23}$-*co*-$AnthGE_9$) during the irradiation at $\lambda = 365$ nm. C) In contrast to the dimerization of 9-methoxymethylanthracene, or $mPEO_{114}$-*b*-P($EHGE_{23}$-*co*-$AnthGE_9$) in DCM solution, the dimerization can be described best by a second order rate law ($A_{rel} = A/A_0$, $\lambda = 369$ nm). D) Comparison of ^{1}H NMR spectra of the diblock terpolymer after irradiation ($\lambda = 365$ nm) in DCM solution ($c = 3$ mg mL^{-1}, dark blue), and after irradiation of micelles in aqueous solution (1 mg mL^{-1}), indicate that the two processes do not lead to the same product.

solution structure upon crosslinking (Figure S11, Supporting Information). Nevertheless, analysis of the reaction kinetics revealed that a second order rate law was more suitable to describe the micellar crosslinking reaction than a first order rate law (Figure 6C). As discussed subsequently, this may hint towards a different reaction mechanism, or an overall different reaction occurring in this case. Despite that, successful crosslinking of the micelles was proven via DLS. The surrounding solvent (water) was gradually replaced with THF, which led to disassembly of micelles that were not crosslinked via irradiation at $\lambda = 365$ nm. After crosslinking, no significant changes were detectable upon replacement of the solvent with THF (Figure S12, Supporting Information) for $mPEO_{114}$-*b*-P($EHGE_{27}$-*co*-$AnthGE_{12}$) and $mPEO_{114}$-*b*-P($EHGE_{23}$-*co*-$AnthGE_9$). Yet, it was not possible to stabilize $mPEO_{114}$-*b*-P($EHGE_{11}$-*co*-$AnthGE_3$) micelles via crosslinking, presumably due to the low *DP* of AnthGE.

To investigate reversibility of the crosslinking process and induce anthracene dimer cleavage, the degassed solutions were irradiated at $\lambda = 254$ nm. Nevertheless, UV–vis spectra indicated only slight increase of the anthracene signals (Figure S13, Supporting Information). Disassembly of the core-crosslinked micelles upon addition of THF after irradiation at $\lambda = 254$ nm was not observable in DLS analysis. Therefore, it was assumed that the expected [4+4]-anthracene dimer was not the main product formed during the crosslinking reaction. ^{1}H NMR spectra of core-crosslinked, freeze-dried micelles that were subsequently swollen in $CDCl_3$ supported this assumption: The signals at 8.34 and 7.83 ppm (signal a, Figure 6D) indicate formation of anthraquinone, despite degassing of the solution prior to irradiation. Further, the signal of the aromatic ring protons of the polymeric [4+4]-cycloadduct was located at 6.80 ppm (signal b, Figure 6D). In contrast, the core-crosslinked, freeze-dried micelles exhibited aromatic ring proton signals in between 7.65 and 7.14 ppm (Signal c, Figure 6D), which may be attributed to a different product of the crosslinking reaction.

As polyether structures are flexible and exhibit a higher tendency to allow water molecules to enter and exit the core, it seemed possible that instead of the [4+4]-cycloadduct, the anthracene units were crosslinked forming dihydroxytetrahydrobianthryl compounds upon addition of two water molecules.

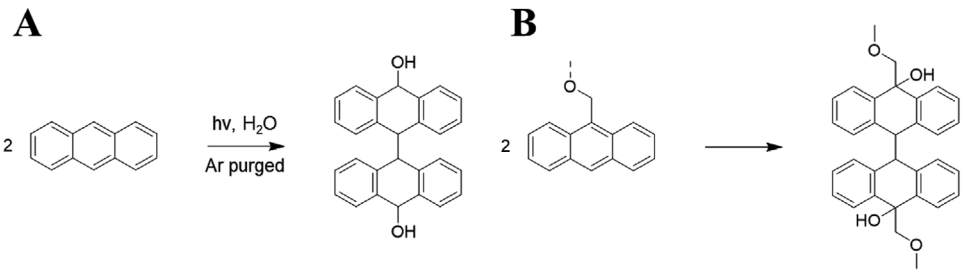

Scheme 3. A) Photolysis, or photochemical dimerization, of anthracene in argon-purged, aqueous solutions, as proposed by Sigman et al.[42] The same reaction type may lead to irreversible crosslinking of polymer-bound anthracene moieties in contact with water.

These species were found as the main products of the irradiation of aqueous, degassed anthracene solutions at $\lambda = 350$ nm by Sigman et al. (**Scheme 3**A).[42] As this crosslinking process, as well as the formation of anthraquinone, is not reversible via irradiation at $\lambda = 254$ nm, no regeneration of the anthracene units and the corresponding UV–vis signal was possible.

The limited mobility and availability of both anthracene units and water molecules is a possible explanation for the reaction order determined for the crosslinking process, though it has to be mentioned that the reaction order of the anthracene [4+4]-cycloaddition can also vary between zero and two, depending on the reaction conditions.[53]

3. Conclusion

In conclusion, we successfully incorporated 9-methylanthracenyl glycidyl ether (AnthGE) into polyether-based diblock terpolymers via AROP. The diblock terpolymers of the structure mPEO-*b*-P(EHGE-*co*-AnthGE) self-assembled into micelles of different morphologies upon rehydration of thin diblock terpolymer films, which were successfully crosslinked via irradiation with UV light at $\lambda = 365$ nm. While the formed dimers can be partially cleaved via irradiation at $\lambda = 254$ nm if the crosslinking reaction was carried out in degassed, organic solution, only small amounts of the anthracene units can be recovered in the case of core-crosslinked micelles in aqueous solutions. ^{1}H NMR and kinetic studies supported the assumption that irreversible dimerization via photo-oxidation and subsequent dimerization upon water addition was instead responsible for micellar crosslinking. Further, the cleavage of the anthracene units from the polymer backbone and the formation of anthraquinone as a side reaction contribute to the rapid decrease of the intensity of the UV–vis signals of anthracene during irradiation of the micelles with UV light ($\lambda =$ 365 nm).

4. Experimental Section

Materials: All starting materials were purchased in analytical grade from Sigma-Aldrich (tetrabutyl ammonium bromide (TBABr), tetrabutyl ammonium iodide (TBAI), 9-anthracenecarboxylic acid, epichlorohydrin, NaH, methyl iodide (MeI)), VWR Chemicals (EtOH, MeOH, THF, ethyl acetate (EtOAc), hexane) J&K Scientific Ltd. ($LiAlH_4$ solution, EHGE), Merck (benzene), or JenKem (mPEO) and were used as received if not mentioned otherwise. The solvent used for anionic polymerization (benzene) was stirred with sodium and benzophenone at room temperature until the blue color of the benzophenone ketyl radical indicated the absence of traces of water. Subsequently, it was distilled from sodium in a still apparatus and stored at room temperature over 3 Å molecular sieves under argon in a glovebox. EHGE was stirred over CaH_2 for at least 24 h, subsequently distilled and stored at −21 °C under argon in a glovebox. AnthGE and the synthesized diblock terpolymers were dried under high vacuum and stored at room temperature under argon in the dark. TBABr was recrystallized from EtOAc and stored dry. Any glassware was cleaned in a KOH/isopropanol bath and dried at 100 °C. All deuterated solvents were obtained from Eurisotop and ABCR.

Methods: SEC was measured on a Shimadzu system equipped with a SCL-10A system controller, a LC-10AD pump, and a RID-10A refractive index detector using a solvent mixture containing chloroform, triethylamine, and isopropanol (94:4:2) at a flow rate of 1 mL min^{-1} on a PSS–SDV–linear M 5 µm column at room temperature. The system was calibrated with PEO (440–44 700 Da) standards.

^{1}H NMR measurements were performed on a 300 MHz Bruker spectrometer using $CDCl_3$ or acetone-d_6 as deuterated solvent. For calibration, the specific signals of the non-deuterated species were used. To calculate the conversion of the dimerization and the dimer cleavage process from ^{1}H NMR spectra, the ratio of dimerized anthracene units to the complete amount of anthracene units (reacted and unreacted) was calculated as follows:

$$\text{Conversion } (mol\%) = \frac{I(b' + c'))/8}{(I(a + b + c)/9) + (I(b' + c')/8)} \quad (1)$$

The letters represent the assigned signals as shown in Figure S4, Supporting Information, for the small molecule compounds, or in Figure 2 for the diblock terpolymer.

DLS measurements were performed on an ALV DLS/SLS equipment consisting of an ALV Laser CGS3 goniometer with an ALV Avalanche correlator and a He—Ne laser ($\lambda = 632.8$ nm). Solvent viscosity and refractive index were automatically adjusted to the temperature of the thermostat. For samples in THF/water mixtures, solvent viscosity and refractive index were calculated from literature values for 298 K. The CONTIN algorithm was applied to analyze the obtained correlation functions. Apparent hydrodynamic radii were calculated according to the Stokes–Einstein equation.

Cryo-transmission electron microscopy (TEM) measurements were performed on a FEI Tecnai G^2 20 cryo-transmission electron microscope. Acceleration voltage was set to 200 kV. Samples were prepared on Quantifoil grids (3.5/1) after cleaning by argon plasma treatment for 120 s. 10 µL of the solutions were blotted by using a Vitrobot Mark IV. The aqueous samples (1 mg mL^{-1}) were plunge-frozen in liquid ethane and stored under nitrogen before being transferred to the microscope utilizing a Gatan transfer stage. TEM images were acquired with a 200 kV FEI Tecnai G^2 20 equipped with a 4k × 4k Eagle HS CCD and a 1k × 1k Olympus MegaView camera. Micrographs were adapted in terms of brightness and contrast using the software ImageJ 1.47v.

UV–Vis measurements were performed on an Agilent (Santa Clara, CA, USA) Cary 60 UV–Vis spectrophotometer with a peltier single cell holder. The measurements in solution were performed in a cuvette (Hellma Optics, Jena, Germany) with a path length of 1 cm.

Fluorescence spectra were recorded on a Jasco FP-8300 spectrofluorometer using glass cuvettes (Hellma Optics, Jena, Germany) with a path length of 1 cm.

Irradiation of the samples was carried out using a 200 W Hg(Xe) lamp from LOT-QuantumDesign (Darmstadt, Germany). UV bandpass filters (Hoya U-360 for irradiation at 365 nm and a traditional-coated UV interference bandpass filter with a CWL of 254 nm for irradiation at 254 nm, Edmund Optics, Karlsruhe, Germany) were used to generate the desired wavelengths.

Linearized fits of the UV–Vis absorption at a specified wavelength for the determination of the reaction order were carried out using the software OriginPro 9.0. Fits were carried out for the reaction orders 0 ($A = A_0 + \nu_A kt$, linearized rate law: A vs t), 1 ($A = A_0 e^{\wedge}(\nu_A kt)$, linearized rate law: ln(A) vs t), 2 ($A = 1/(1/A_0 - \nu_A kt$, linearized rate law: $1/A$ vs t), and 3 ($1/A^2 = 1/A_0{}^2 - 2\nu_A kt$, linearized rate law: $1/A^2$ v t). Pearson's r^2 was maximized. A = Absorption; A_0 = initial absorption; ν_A = stoichiometric number of A; k = rate constant; t = time.

Synthesis of 9-methylanthracenyl Glycidyl Ether (AnthGE, 2-((anthracen-9-ylmethoxy)methyl)oxirane): A suspension of $LiAlH_4$ (2.4 mol L^{-1} in THF, 6 mL, 14.4 mmol) was added to 50 mL of dry THF stirred under argon in a Schlenk flask at 0 °C. Then, 9-anthracenecarboxylic acid (1 g, 2.25 mmol), dissolved in 30 mL of dry THF, was added dropwise to the solution. The ice-bath used for cooling was removed after addition and the reaction mixture was stirred for 24 h while warming to room temperature. Then, the reaction mixture is again cooled to 0 °C and excess $LiAlH_4$ is quenched by dropwise addition of 10 mL of 1 N aqueous KOH. Subsequently, THF was removed under reduced pressure and the resulting mixture was extracted with diethyl ether (3 × 30 mL). The combined organic phases were washed with 1 N HCl (1×, 40 mL) and brine (1×, 40 mL), dried over Na_2SO_4, filtered and the solvent was removed under reduced pressure to yield 9-anthracenemethanol (910 mg, 4.36 mmol, 97%) as light yellow solid. The product was used in the next step without further purification.[57]

^{1}H NMR (300 MHz, Acetone-d_6, δ): 8.55 (d, J = 4.2 Hz, 2H, C—C—C*H* (Aryl)), 8.51 (s, 1H, C—C*H*—C (Aryl)), 8.14–8.06 (m, 2H, C—C*H* (Aryl)), 7.63–7.48 (m, 4H, C*H*—C*H* (Aryl)), 5.63 (s, 2H, CH_2—OH).

In the next step, a 20 mL microwave vial was charged with 9-anthracenemethanol (800 mg, 3.84 mmol), KOH (430 mg, 7.68 mmol), a catalytic amount of TBABr and 6 mL of dry THF. The vessel was sealed and degassed with argon for 10 min before epichlorohydrin (1.5 mL, 19.2 mmol) was added via syringe. The vial was then heated to 75 °C for 24 h under stirring. After cooling to room temperature, the solution was filtered and the residue was washed with THF. The solvent was then removed under reduced pressure and the crude product was adsorbed onto silica gel and purified via column chromatography ($CHCl_3$/EtOAc 98:2). The product fraction was dried under reduced pressure and subsequently recrystallized from Toluene/EtOH to yield the pure product (520 mg, 1.96 mmol, 51%) as light yellow crystals.[58,59]

^{1}H NMR (300 MHz, $CDCl_3$, δ): 8.50 (s, 1H, C—C*H*—C (Aryl)), 8.47–8.40 (m, 2H, C—C—C*H* (Aryl)), 8.04 (d, J = 8.3 Hz, 2H, C—C*H* (Aryl)), 7.54 (dddd, J = 9.4, 7.7, 6.5, 1.2 Hz, 4H, C*H*—C*H* (Aryl)), 5.60 (q, J = 11.5 Hz, 2H, C—CH_2—O), 3.95 (dd, J = 11.6, 3.0 Hz, 1H, O—CH_2—CH), 3.64 (dd, J = 11.6, 5.7 Hz, 1H, O—CH_2—CH), 3.25 (ddt, J = 5.7, 4.1, 2.8 Hz, 1H, C*H* (Epoxide)), 2.87–2.76 (m, 1H, CH_2 (Epoxide)), 2.66 (dd, J = 5.0, 2.7 Hz, 1H, CH_2 (Epoxide)).

Synthesis of 9-Methoxymethylanthracene: 9-Anthracenemethanol (500 mg, 2.3 mmol) was dissolved in 8 mL of dry THF under argon. Then, the solution was cooled to 0 °C and NaH (60% in mineral oil, 185 mg, 4.6 mmol) was added. Stirring was continued for 30 min before MeI (290 µL, 4.6 mmol) and TBAI (86 mg, 0.23 mmol) were added. Stirring was continued for 18 h while the reaction was allowed to warm to room temperature. Subsequently, the reaction was quenched by adding 2 mL of MeOH. The reaction mixture was diluted with ethyl acetate (50 mL), and the organic phase was washed with water (50 mL, 1×), and brine (50 mL, 2×). Afterward, the organic phase was dried over Na_2SO_4, the solvent was evaporated under reduced pressure, and the crude product was recrystallized from a mixture of hexane and EtOH (4:1) to yield 331 mg (1.5 mmol, 65%) of pure 9-methoxymethylanthracene as yellow crystals.[60]

^{1}H NMR (300 MHz, $CDCl_3$, δ): 8.49 (s, 1H, C—C*H*—C (Aryl)), 8.41 (d, J = 8.1 Hz, 2H, C—C—C*H* (Aryl)) 8.04 (d, J = 8.1 Hz, 2H, C—C*H* (Aryl)), 7.54 (dddd, J = 9.4, 7.7, 6.5, 1.2 Hz, 4H, C*H*—C*H* (Aryl)), 5.47 (s, 2H, CH_2), 3.57 (s, 3H, CH_3).

Synthesis of the Diblock Terpolymers: For block extension of commercially available mPEO–OH, the macroinitiator was dissolved in dry benzene at a concentration of 30 mg mL^{-1} in a microwave vial under argon in a glove box. A catalytic amount of NaH was added, the reaction vessel was sealed and the mixture was heated at 110 °C under stirring for 2 h. Then, the desired amount of monomer (EHGE and AnthGE) was dissolved in a small amount of dry benzene and added to the reaction mixture. For $mPEO_{114}$-*b*-P($EHGE_{27}$-*co*-$AnthGE_{12}$) and $mPEO_{114}$-*b*-P($EHGE_{23}$-*co*-$AnthGE_9$), 225 µL of EHGE and 100 mg of AnthGE were used for the block extension of 100 mg of mPEO-OH. For $mPEO_{114}$-*b*-P($EHGE_{11}$-*co*-$AnthGE_3$), 150 µL of EHGE and 65 mg of AnthGE were used per 100 mg of mPEO-OH. Stirring at 110 °C was continued for 48 h before the reaction was quenched by addition of 1 mL of EtOH. The solution was filtered through a glass fiber filter (1 µm pore size) after cooling to remove NaOH, and the solvent was removed under reduced pressure. The yield of crude product was between 90% and 95%, calculated by weight. Residual monomer that was left in the reaction solution due to incomplete conversion as well as low molecular weight byproducts were removed via dialysis against THF using RC membranes (MWCO = 6000–8000 kDa). The yield of the purified polymers was 75% calculated by weight and varied slightly with the reaction batch. The polymers were stored in the dark until use.[21]

Please note that the authors only used benzene, as common substitutes such as toluene resulted in significantly lower degrees of polymerization. As benzene is carcinogenic, it has to be ensured that emission of benzene to the laboratory atmosphere is prevented.

^{1}H NMR (300 MHz, $CDCl_3$, δ): 8.31 (s, br, 3H, anthracene), 7.89 (s, br, 2H, anthracene), 7.39 (s, br, 4H, anthracene), 5.35 (s, br, 2H, anthracene-CH_2), 4.03–2.91 (m, polymer backbone), 1.44 (s, 1H, 2-ethylhexyl-C*H*), 1.27 (m, 8H, 2-ethylhexyl-CH_2), 0.87 (m, 6H, 2-ethylhexyl-CH_3).

Micellization: For micellization, the polymers were dissolved in THF (10 mg mL^{-1}) in a glass vial. Then, THF was evaporated under reduced pressure to form a thin diblock terpolymer film. This film was subsequently rehydrated in micropure water at a concentration of 1 mg mL^{-1} via stirring for three days. This method allows for the generation of micellar structures without residual solvent, as it may be the case if the solvent switch method is used. Pre-ordering of the diblock terpolymers in the thin polymer film may influence the resulting solution structure.[22,61] Crosslinking procedures for the micelles are described within the results and discussion section.

Supporting Information

Supporting Information is available from the Wiley Online Library or from the author.

Acknowledgements

The authors thank the German Research Council (DFG) for financial support of the project (SCHA 1640/16-1 and Project B05 within the Sonderforschungsbereich SFB/TRR 234"CataLight", project ID: 364549901). The cryo-TEM/TEM facilities of the Jena Center for Soft Matter (JCSM) were established with a grant from the German Research Council (DFG) and the European Funds for Regional Development (EFRE).

Open access funding enabled and organized by Projekt DEAL.

Conflict of Interest

The authors declare no conflict of interest.

Data Availability Statement

Research data are not shared.

Keywords

anthracene, core-crosslinking, light-induced crosslinking, polymeric micelles

Received: July 26, 2021
Revised: August 23, 2021
Published online: September 13, 2021

[1] H. Cabral, K. Miyata, K. Osada, K. Kataoka, *Chem. Rev.* **2018**, *118*, 6844.
[2] B. Louage, M. J. Van Steenbergen, L. Nuhn, M. D. P. Risseeuw, I. Karalic, J. Winne, S. Van Calenbergh, W. E. Hennink, B. G. De Geest, *ACS Macro Lett.* **2017**, *6*, 272.
[3] D. Leroy, L. Martinot, C. Jérôme, R. Jérôme, *J. Radioanal. Nucl. Chem.* **1999**, *240*, 867.
[4] L. Volkmann, M. Köhler, F. H. Sobotta, M. T. Enke, J. C. Brendel, F. H. Schacher, *Macromolecules* **2018**, *51*, 7284.
[5] M. T. De Martino, L. K. E. A. Abdelmohsen, F. P. J. T. Rutjes, J. C. M. Van Hest, *Beilstein J. Org. Chem.* **2018**, *14*, 716.
[6] Y. Liu, Y. Wang, Y. Wang, J. Lu, V. Piñón, M. Weck, *J. Am. Chem. Soc.* **2011**, *133*, 14260.
[7] M.-O. Simon, C.-J. Li, *Chem. Soc. Rev.* **2012**, *41*, 1415.
[8] A. O. Moughton, M. A. Hillmyer, T. P. Lodge, *Macromolecules* **2012**, *45*, 2.
[9] O. W. Webster, *Science* **1991**, *251*, 887.
[10] K. Matyjaszewski, *Controlled/Living Radical Polymerization*, American Chemical Society, **2000**, p. 2.
[11] F. Le Devedec, A. Won, J. Oake, L. Houdaihed, C. Bohne, C. M. Yip, C. Allen, *ACS Macro Lett.* **2016**, *5*, 128.
[12] J. Herzberger, K. Niederer, H. Pohlit, J. Seiwert, M. Worm, F. R. Wurm, H. Frey, *Chem. Rev.* **2016**, *116*, 2170.
[13] Y. Shao, W. Huang, C. Shi, S. T. Atkinson, J. Luo, *Ther. Delivery* **2012**, *3*, 1409.
[14] Y. Lu, Z. Yue, J. Xie, W. Wang, H. Zhu, E. Zhang, Z. Cao, *Nat. Biomed. Eng.* **2018**, *2*, 318.
[15] X. Jiang, B. Zhao, *Macromolecules* **2008**, *41*, 9366.
[16] J. Ren, Y. Zhang, J. Zhang, H. Gao, G. Liu, R. Ma, Y. An, D. Kong, L. Shi, *Biomacromolecules* **2013**, *14*, 3434.
[17] M. Talelli, M. Barz, C. J. F. Rijcken, F. Kiessling, W. E. Hennink, T. Lammers, *Nano Today* **2015**, *10*, 93.
[18] T. Rudolph, F. H. Schacher, *Eur. Polym. J.* **2016**, *80*, 317.
[19] J. Morsbach, J. Elbert, C. Rüttiger, S. Winzen, H. Frey, M. Gallei, *Macromolecules* **2016**, *49*, 3406.
[20] B. Zhang, X. Lv, A. Zhu, J. Zheng, Y. Yang, Z. An, *Macromolecules* **2018**, *51*, 2776.
[21] J. K. Elter, G. Sentis, P. Bellstedt, P. Biehl, M. Gottschaldt, F. H. Schacher, *Polym. Chem.* **2018**, *9*, 2247.
[22] J. K. Elter, S. Quader, J. Eichhorn, M. Gottschaldt, K. Kataoka, F. H. Schacher, *Biomacromolecules* **2021**, *22*, 1458.
[23] M. J. Barthel, T. Rudolph, S. Crotty, F. H. Schacher, U. S. Schubert, *J. Polym. Sci., Part A: Polym. Chem.* **2012**, *50*, 4958.
[24] X. Xu, J. D. Flores, C. L. Mccormick, *Macromolecules* **2011**, *44*, 1327.
[25] C. Sun, H. Jia, K. Lei, D. Zhu, Y. Gao, Z. Zheng, X. Wang, *Polymer* **2019**, *160*, 246.
[26] G. Wang, X. Tong, Y. Zhao, *Macromolecules* **2004**, *37*, 8911.
[27] H.-I. Lee, W. Wu, J. K. Oh, L. Mueller, G. Sherwood, L. Peteanu, T. Kowalewski, K. Matyjaszewski, *Angew. Chem., Int. Ed.* **2007**, *46*, 2453.
[28] O. Grimm, S. C. Maßmann, F. H. Schacher, *Polym. Chem.* **2019**, *10*, 2674.
[29] Y. Zhao, *Macromolecules* **2012**, *45*, 3647.
[30] J. Jiang, B. Qi, M. Lepage, Y. Zhao, *Macromolecules* **2007**, *40*, 790.
[31] X. Yuan, K. Fischer, W. Schärtl, *Langmuir* **2005**, *21*, 9374.
[32] S. Guan, A. Chen, *ACS Macro Lett.* **2020**, *9*, 14.
[33] W. Wen, T. Huang, S. Guan, Y. Zhao, A. Chen, *Macromolecules* **2019**, *52*, 2956.
[34] S. Mototaro, *Bull. Chem. Soc. Jpn.* **1943**, *18*, 146.
[35] H. Bouas-Laurent, J.-P. Desvergne, A. Castellan, R. Lapouyade, *Chem. Soc. Rev.* **2000**, *29*, 43.
[36] H. Bouas-Laurent, J.-P. Desvergne, A. Castellan, R. Lapouyade, *Chem. Soc. Rev.* **2001**, *30*, 248.
[37] M. J. Barthel, T. Rudolph, A. Teichler, R. M. Paulus, J. Vitz, S. Hoeppener, M. D. Hager, F. H. Schacher, U. S. Schubert, *Adv. Funct. Mater.* **2013**, *23*, 4921.
[38] Z.-C. Jiang, Y.-Y. Xiao, X. Tong, Y. Zhao, *Angew. Chem., Int. Ed.* **2019**, *58*, 5332.
[39] S. Telitel, E. Blasco, L. D. Bangert, F. H. Schacher, A. S. Goldmann, C. Barner-Kowollik, *Polym. Chem.* **2017**, *8*, 4038.
[40] P. G. Frank, B. T. Tuten, A. Prasher, D. Chao, E. B. Berda, *Macromol. Rapid Commun.* **2014**, *35*, 249.
[41] C. Liu, Y.-Y. Fei, H.-L. Zhang, C.-Y. Pan, C.-Y. Hong, *Macromolecules* **2019**, *52*, 176.
[42] M. E. Sigman, S. P. Zingg, R. M. Pagni, J. H. Burns, *Tetrahedron Lett.* **1991**, *32*, 5737.
[43] R. Debestani, K. J. Ellis, M. E. Sigman, *J. Photochem. Photobiol., A* **1995**, *86*, 231.
[44] H. Xie, M.-J. He, X.-Y. Deng, L. Du, C.-J. Fan, K.-K. Yang, Y.-Z. Wang, *ACS Appl. Mater. Interfaces* **2016**, *8*, 9431.
[45] Y. Liu, H. Chang, J. Jiang, X. Yan, Z. Liu, Z. Liu, *RSC Adv.* **2014**, *4*, 25912.
[46] T. Nishiuchi, S.-Y. Uno, Y. Hirao, T. Kubo, *J. Org. Chem.* **2016**, *81*, 2106.
[47] J. Van Damme, O. Van Den Berg, J. Brancart, L. Vlaminck, C. Huyck, G. Van Assche, B. Van Mele, F. Du Prez, *Macromolecules* **2017**, *50*, 1930.
[48] J. Van Damme, O. Van Den Berg, J. Brancart, G. Van Assche, F. Du Prez, *Tetrahedron* **2019**, *75*, 912.
[49] S. Hocine, M.-H. Li, *Soft Matter* **2013**, *9*, 5839.
[50] S. Ikuta, *J. Mol. Struct.: THEOCHEM* **2000**, *530*, 201.
[51] M. Hans, H. Keul, M. Moeller, *Polymer* **2009**, *50*, 1103.
[52] A. Kislyak, H. Frisch, M. Gernhardt, P. H. M. Van Steenberge, D. R. D'hooge, C. Barner-Kowollik, *Chem. - Eur. J.* **2020**, *26*, 478.
[53] A. Kislyak, D. Kodura, H. Frisch, F. Feist, P. H. M. Van Steenberge, C. Barner-Kowollik, D. R. D'hooge, *Chem. Eng. J.* **2020**, *402*, 126259.
[54] Z. Machatová, Z. Barbieriková, P. Poliak, V. Jančovičová, V. Lukeš, V. Brezová, *Dyes Pigm.* **2016**, *132*, 79.
[55] E. A. Chandross, J. Ferguson, E. G. Mcrae, *J. Chem. Phys.* **1966**, *45*, 3546.
[56] Y. M. Lopatkin, P. A. Kondratenko, I. P. Zharkov, *Theor. Exp. Chem.* **2001**, *37*, 84.
[57] T. H. West, D. M. Walden, J. E. Taylor, A. C. Brueckner, R. C. Johnston, P. H.-Y. Cheong, G. C. Lloyd-Jones, A. D. Smith, *J. Am. Chem. Soc.* **2017**, *139*, 4366.
[58] A.-L. Zhang, Z.-D. Yu, L.-W. Yang, N.-F. Yang, *Tetrahedron: Asymmetry* **2015**, *26*, 173.
[59] B. Yu, X. Jiang, J. Yin, *Soft Matter* **2011**, *7*, 6853.
[60] A. M. Sarotti, R. A. Spanevello, A. G. Suárez, *Tetrahedron* **2009**, *65*, 3502.
[61] J. K. Elter, P. Biehl, M. Gottschaldt, F. H. Schacher, *Polym. Chem.* **2019**, *10*, 5425.

